The effect of close post injection on combustion characteristics and cooling loss reduction

Zhichao Bao [a,*], Ryo Kishigami [a], Naoto Horibe [a], Hiroshi Kawanabe [a], Takuji Ishiyama [a]
[a] Graduate School of Energy Science, Kyoto University, Yoshida-honmachi, Kyoto, Japan
* Corresponding author. Email address: bao.chishao.64z@st.kyoto-u.ac.jp

Abstract

In previous study, post injection has shown a significant benefit in the reduction of soot emissions. Among them, the close post injection which only has short dwell between the main injection is supposed to be able to increase the thermal efficiency. The reduction of the cooling loss due to the main flame impingement is considered as the reason to the increase of thermal efficiency. However, there is a lack of study related to the influence of post injection timing and quantity on the combustion characteristics. Therefore, in this study, the engine performance and emission characteristics of injection strategy with close post injection was investigated. The post injection timing was modified from near zero interval to around 4.5°CA from the end of main injection. In addition, the post injection quantity was modified from 3, 9, to 15 mm^3/cycle and the intake pressure was modified from 170, 200, to 220 kPa while maintaining the total injection quantity at 39 mm^3/cycle. In order to clarify the mechanism of cooling loss by applying post injection and the effect of injection dwell to the cooling loss and combustion characteristics, an optical engine was used to observe the combustion process. As a result, a certain dwell is needed to fully exploit the effect of cooling loss reduction by post injection.

Keywords: Diesel engine; Post injection; Multi-injection; Cooling loss; Spray combustion

1. Introduction

Traditionally the NOx and soot emissions were the two main concerns for diesel engine and they were strictly restricted [1]. For the reduction of NOx, the exhaust gas recirculation (EGR) technology was widely researched and applied to modern diesel engines [2]. As for the soot reduction, one of the solutions is post injection which reduces main injection quantity and plus an additional injection after main injection. This multiple injection strategy was achieved by the development of common-rail system and injector system [3, 4]. As a result, more complex injection strategies could be applied with faster response to reduce harmful emissions as well as combustion noises [5, 6]. Previous researches indicated that the post injection duration, timing were significant factors affecting the efficacy of post injection on soot and UHC emissions [5]. Some studies stated that the mechanism of the soot emissions reduction is due to the reduction of main injection quantity [7, 8]. Those researches claimed that less main injection quantity leads to lower soot formation by main combustion, and the post injection does not produce significant additional soot emissions. Therefore, global soot emissions were suppressed. As for the post injection timing, in summary, there are two possible scenarios in which a post injection seems to be an efficient strategy to reduce soot emissions. One is when the post injection is very close to the main injection and the other is when it is far enough from the main injection [7-12]. The researches on far post injection, the post injection with a certain gap between the main injection, indicated that the lower temperature of the unburned gas at the end of post injection prevents the formation of soot. On the other hand, the close post injection implies that the application of post injection accelerated the final stage of combustion which makes the soot oxidization occurs at higher temperature [12].

Although the post injection has significant advantages on emission reduction mentioned above, the total combustion duration will be extended by dividing main injection into main and post injection. As a result, the degree of constant volume (DCV) may drop and thermal efficiency will decrease. Therefore, from the perspective of thermal efficiency, the gap between main and post injection should be minimized [8, 12, 13]. Moreover, recently, some studies indicate that the short interval injection could have the effect of reducing cooling loss [8, 14, 15]. The explanation to this phenomenon is the reduction of the high temperature gas quantity and motion near the combustion chamber wall. Hence, instead of deteriorating the thermal efficiency, applying the close post injection is possible to achieve higher fuel economy.

According to these theories, a larger amount of post injection could decrease more cooling loss by suppressing the main injection impingement but, in turn, the DCV could reduce. Therefore, there may exist a tradeoff relationship between the improvement of thermal efficiency by decreasing cooling loss and the reduction of thermal efficiency by the decrease of DCV when a certain amount of close post injection is applied.

Moreover, it is reported that when post injection was applied to heavy-duty diesel engines with low temperature combustion operating conditions, the fluid interaction between main injection and post injection mixture will help to reduce the unburnt hydrocarbon emission [16, 17]. In addition, the transient process associated with the small post injection is reported to have a positive effect on thermal efficiency [12]. These results indicate that the interaction between the main and post injection spray could affect the combustion characteristics of the close post injection. However, there is limited data concerned about the near zero interval of main and post injection.

Therefore, in this study, a metal engine was used to investigate the effect of close post injection on engine performance. The injection timing of the post injection was modified so that it could range from near zero interval with the main injection to a short interval between the main injection. Also, the effects of post injection quantity and intake pressure on engine performance and combustion characteristics were discussed. The results show that the cooling loss could be reduced by applying close post injection. In addition, by retarding post injection timing slightly from near zero interval, the cooling loss showed a minimum. Furthermore, the reason for the effects of injection interval was discussed based on the results of spray and flame visualization using an optical engine.

2. Experimental Setup

2.1 Engine setup and analytical method

The schematic of the single cylinder engine system used for engine performance experiments is shown in Figure 1 and its major specifications are summarized in Table 1. The supercharging system is driven separately from the engine. Therefore, the intake pressure could be changed regardless of the engine rotational speed and engine load. In this series of experiments, the effect of near zero interval post injection on cooling loss and engine performance was investigated at high load condition. Therefore, a high thermal efficiency point was selected with a rotational speed of 2250 rpm and gross indicated mean effective pressure at around 1.4 MPa. The detailed experimental setups were decided as shown in Table 2. The injection pressure (p_j) was measured at common-rail and its value was fixed at 270 MPa through this study. The intake and exhaust pressure were set at the same level to exclude the influence of pumping loss to the experimental results as possible as we could. An intercooler and a heater were used to keep the intake temperature at 50°C. Exhaust pressure could be modified by the back pressure valve and an exhaust chamber was used to minimize the influence of exhaust pressure fluctuation. The exhaust gas could be reintroduced to the intake port through an EGR valve so the EGR rate could be modified by EGR valve aperture. In this study, low pressure EGR system was used. Low pressure EGR system with DPF filter could avoid the contamination of the engine and lubrication oil with soot. Intake oxygen concentration was set to 19.2% by regulating the EGR rate. The piston bowl shape is shown in Figure 2.

A common-rail system and a piezo injector with an injection angle of 156° were used. The nozzle hole number was 12 and its diameter was 0.114 mm. The commercial JIS (Japanese Industry Standard) No.2 diesel fuel (Cetane index 54) was used. The fuel density at 15°C was 839.7 kg/m^3 and the lower heating value was 43.1 MJ/kg. An exhaust gas analyzer (Horiba MEXA 1700DEGR) was used to measure the NOx, total hydrocarbon (THC), CO, CO2, and O2 concentrations while the smoke emissions were obtained by AVL 415S smoke meter.

For metal engine experiments, the heat release rates were calculated from averaging the in-cylinder pressure histories of consequent 50 cycles recorded by an in-cylinder pressure sensor (Kistler 6052C). The cooling loss is calculated by subtracting indicated work, unburned loss, and exhaust loss from input energy. The rate of exhaust loss was calculated by subtracting intake enthalpy from exhaust enthalpy. The heat release rate with compensation of cooling loss was used for DCV calculation.

The schematics of the optical engine are shown in Figure 3 and the cross section view of the combustion chamber is shown in Figure 4. The intake and exhaust system were the same as the metal engine. Optical access is provided through a Bowditch type piston [18]. Its combustion chamber had a diameter of 51.8 mm and a depth of 12.8 mm.

Due to the mechanical limitation of the optical engine, its compression ratio was 15.4 and the rotational speed was set to 2000 rpm. In order to simulate almost the same spray development against crank angle, injector with a nozzle diameter of 0.104 mm was used. The nozzle hole number was unchanged. The intake temperature and intake pressure were maintained at 50°C and 200 kPa, respectively. The operation parameters are summarized and compared with that of metal engine in Table 2. In this study, the equation presented by Wakuri was used to predict the spray tip penetration [19].

$$x = C \cdot (\frac{\Delta p}{\rho_a})^{1/4} \cdot (\frac{d_0 t}{\tan\theta})^{1/2}$$

x: spray tip penetration;

C: model constant;

Δp: difference of injection pressure and ambient pressure;

ρ_a: ambient density;

θ: half cone angle of the fuel spray;

d_0: nozzle diameter;

t: time from start of injection;

The Δp is approximately proportional to injection pressure, and the ratio of ρ_a can be calculated by the ratio of compression ratio and intake pressure. With the operation parameter setup listed in Table 2, the ratio of spray tip penetration as a function of time for metal and optical engine is equal to 1.143. Since the ratio of rotational speed is 1.125, the ratio between the crank angle resolved penetration of metal and optical engine was approximately 1. It should also be noted that the spray tip velocity when it reaches the rim of the chamber is different since the diameter of the bowl is different.

A high speed camera (Photron FASTCAM SA-Z) was used for the optical experiments. The frame rate was 60,000 fps which correspond to 1 picture per 0.2 °CA. The picture size was 384 x 728 pixel and its resolution was 0.1 mm/pixel. During the optical engine experiments, the injection process only occurred for 7 consecutive cycles. The calculated heat release rates of each cycle were compared with the average heat release rate of 7 cycles. Due to the influence of residual gas, the history of in-cylinder pressure was different between the first cycle and the last cycle. In this study, since the history of in-cylinder pressure of the 5th cycle was closest to the average in-cylinder pressure history, it was chosen as the representative when comparing the optical results.

2.2 Injection timing setting

Usually, the injection patterns of diesel engine at high load conditions include several pilot injections. Two-stage pilot injection is widely applied to suppress the combustion noise and emissions. The target of this study is the investigation of the characteristics of close post injection when it is applied to a normal injection pattern. Therefore, in this series of study, a two-stage pilot injection was applied before the main injection. The injection timing was set at -20.2 and -9.2 °ATDC, respectively. And their injection quantities were 1.7 and 1.8 mm^3/cycle. The main injection timing was fixed at -1.7 °ATDC and the post injection timing, which was a vital parameter, was changed to modify the interval between main injection and post injection. The total injection quantity was 39 mm^3/cycle while the post injection quantity was set to be 0, 3, 9, and 15 mm^3/cycle. The injection parameters mentioned above are summarized in Table 3.

The injection rate was measured by using the Zeuch type injection rate meter (Onosokki FJ7000) and 12.5 kHz low pass filter was applied to the original pressure signal to remove the noise signals. The experiment parameters with 0, 3, 9, and 15 mm^3/cycle were named as ppM, ppMP3, ppMP9, and ppMP15, respectively. As references, the experiments without post injection (post injection quantity was reduced from main injection quantity) were also conducted and they were referred to as ppM(P3), ppM(P9), and ppM(P15). The number in brackets referred to the injection quantity reduced from the main injection compared to ppM. For each post injection quantity, the injection timing of the post injection was also modified. Take injection rate results with post injection quantity of 9 mm^3/cycle as an example, as shown in Figure 5, the interval of the injection timing ($\Delta\theta$) between main and post injection was determined as the interval of the intercept of the fitted lines of the injection rate of the end of main injection and the start of post injection. For each post injection quantity, 4 patterns of the interval were selected and they are summarized in Table 4. The $\Delta\theta$ are added at the last of the experiment label. In addition, the relative locations of the injection axis to the chamber wall are shown in Figure 6 as a reference.

The injection rates with various post injection quantity and timing are shown from Figure 7 to Figure 9. With the decrease of post injection quantity, the maximum main injection rate decreased. In addition, when post injection quantity was 3 and 9 mm^3/cycle, the maximum injection rates were lower than main injection. On the other hand, the maximum injection rate of the post injection was almost the same with the main injection when post injection quantity was 15 mm^3/cycle. When post injection quantity was 9 and 15 mm^3/cycle, the maximum post injection rate increased slightly with the retard of post injection timing.

For optical experiments, since the rotational speed was different from the metal engine operation condition, the injection timing and duration instead of the injection quantity was set to be the same compared to metal engine operating conditions. The examples of the comparison of injection rate for optical engine and metal engine with $\Delta\theta$ of 0°CA and 3.2°CA are shown in Figure 10. For the optical experiments (labeled with ppMP6), we aimed to adjust the same injection duration with the metal engine experiments. So the total injection quantity and post injection quantity were different from metal engine experiments. Though the ratios of injection quantity between two pilot injections and main injection were also not exactly the same compared to metal engine operating condition, the interval between main and post injection, which was the main concern of the optical experiments, was adjusted to be the same.

However, the differences in the fuel rate shown in Table 2 and the fuel rate ratio between main and post injection shown in Figure 10 indicate that the injection rate of main injection was much lower for optical experiments compared to metal engine experiments. In other words, the heat release of main injection may take a lower proportion for optical experiments than actual metal engine operation conditions. Therefore, the injection parameters of the optical experiments had the same injection interval as ppMP9 of metal engine experiments, but the heat input ratios of main and post injection were more close to ppMP15 of metal engine experiments. In addition, if we also consider that the actual bore size is smaller for optical engine, the interaction of fuel spray with the chamber wall was exaggerated compared to that of main flame.

3. Metal engine experiment results and discussion

3.1 The effect of post injection timing

Figure 11 shows the results of the average in-cylinder temperature (T), in-cylinder pressure (p), heat release rate ($\mathrm{d}Q/\mathrm{d}\theta$), and injection rate with post injection quantity of 9 mm^3/cycle. The results of ppM and ppM(P9) are also shown in the figures as references. As a whole, two-stage heat release followed the pilot injections before top dead center (TDC) and the main heat release occurred around TDC. The peak of the main heat release and the maximum in-cylinder pressure decreased by applying post injection. In addition, the highest in-cylinder pressure decreased with the retard of post injection timing.

The engine performance results are shown in Figure 12 and the emission results are shown in Figure 13. Figure 12 shows that the cooling loss could be decreased by applying post injection with the range of $\Delta\theta$ from 0°CA to 5°CA. The cooling loss could be further reduced by slightly retarding post injection timing from 0°CA interval to around 1.5°CA. However, when the post injection timing was further retarded, the cooling loss did not continue to drop. Instead, it increased slightly.

In summary, as shown in Figure 12, the thermal efficiency increased by applying close post injection. This is because of the decrease of cooling loss while maintaining approximately the same DCV compared with ppM condition. When the $\Delta\theta$ was retarded from 0°CA to 1.5°CA, the thermal efficiency increased with the decrease of cooling loss. Moreover, when $\Delta\theta$ is further retarded from 1.5°CA the thermal efficiency showed a decrease due to the increase of cooling loss. Therefore, the thermal efficiency is strongly related to the cooling loss ratio in this series of experiments.

According to Figure 13, the THC, CO, and smoke emissions levels were low when three-stage injection (ppM) was applied. Post injection strategy, as well as its timing, seemed to have little effect on THC and CO emissions. The smoke emissions increased slightly by increasing post injection quantity. Compared with ppM, NOx emission increased by applying post injection and decreased with the retard of post injection timing.

3.2 The effect of post injection quantity

In the next step, the effect of post injection quantity on the engine performance and exhaust emissions were investigated. The post injection quantity was modified to 3 and 15 mm^3/cycle. The results of T, p, $\mathrm{d}Q/\mathrm{d}\theta$, and injection rates are shown in Figure 14 and

Figure 15. The results of engine performance and exhaust emissions are summarized together with the results of ppMP9 in Figure 16 and Figure 17.

With post injection quantity of 3 mm^3/cycle, almost no differences in the maximum in-cylinder pressure were observed with various post injection timing. On the other hand, with post injection quantity of 15 mm^3/cycle, the maximum in-cylinder pressure was reduced by applying post injection and it was further reduced by retarding post injection timing. These results were the same with post injection quantity of 9 mm^3/cycle. In addition, with post injection quantity of 15 mm^3/cycle, the timing of maximum heat release rate retarded by applying post injection of 0°CA interval and it was further retarded by retarding post injection timing.

The cooling loss showed the same trend with the results with post injection quantity of 9 mm^3/cycle (Figure 16). In other words, the cooling loss reduced and reached the minimum level when $\Delta\theta$ was around 1°CA to 2°CA. Then, the cooling loss showed an increase with the further retarding of post injection timing. The DCV decreased with the increase of injection quantity. As a result, the larger post injection quantity led to lower thermal efficiency. However, overall, when close post injection was applied, the thermal efficiency was higher compared to ppM. According to Figure 17, the smoke emission was at a low level through this series of experiments and the NOx emission decreased when post injection timing was retarded.

3.3 The effect of intake pressure

In this series of experiments, the intake pressure was modified to investigate the effect of in-cylinder density on cooling loss reduction by post injection. The injection pressure was unchanged with the previous experiments while the intake pressure was modified from 170, 200, to 220 kPa. The injection parameters of ppMP9_0 and ppMP9_4.7 are chosen as examples and their results of T, p, $\mathrm{d}Q/\mathrm{d}\theta$, and injection rates are shown in Figure 18 and Figure 19. The results of engine performance are shown in Figure 20. Though, higher intake pressure led to slightly higher heat release of post injection, the overall heat release rate shape showed little differences with various intake pressure.

When intake pressure was reduced to 170 kPa, the minimum value of cooling loss was also detected with $\Delta\theta$ around 1°CA. When intake pressure was increased to 220 kPa, the effect of post injection application and $\Delta\theta$ on cooling loss was gentle.

In this series of experiments, the post injection did not significantly reduce the DCV. The thermal efficiency showed a common trend reaching a maximum value with a certain $\Delta\theta$. When the intake pressure was high, the reduction of cooling loss due to post injection was small. Therefore, the effect of thermal efficiency improvement was small.

4. Optical engine experiment results and discussion

The optical engine experiments were conducted to investigate the mechanism of the engine performance and emission characteristics. As mentioned in the experimental setup section, the rotational speed was reduced from 2250 rpm to 2000 rpm due to the mechanical limitation. Therefore, the injection timing and duration instead of the injection quantity was kept for the same with metal engine operating condition. In addition, most importantly, the spray tip development as the function of crank angle was controlled to match with metal engine experiments.

Half of the combustion chamber was visualized during the experiments and 1/4 of the chamber was shown in this section. One example of the optical results is illustrated in Figure 21, which shows the position of the injector nozzle tip and rim of the combustion chamber bowl. The dense part which is a high density region of droplets of the diesel spray and the luminous flame could be observed in the optical results.

At first, we would like to investigate the effect of main injection reduction on flame development, therefore, the optical results of ppM and ppM(P6) were compared in Figure 22 from the start of main injection. In Figure 22 the main injection started at −1.0°ATDC and main flame could be observed from 0.6°ATDC. Then, the spray flame penetrated through the combustion chamber and reached the bowl rim at around 3.8°ATDC. The main injection finished around 5.4°ATDC for ppM(P6) while the main injection lasted until 6.2°ATDC for ppM. With longer main injection duration, the ppM had a larger area of flame and it stayed for longer duration at the periphery of the combustion chamber.

The $\Delta\theta$ could also affect the combustion characteristics. When the $\Delta\theta$ is nearly zero, the spray of main and post injection are supposed to have some interaction with each other. In Figure 23, the optical results of ppM(P6) and ppMP6_0 are compared. Compared with ppM(P6), a 6 mm^3/cycle post injection was added to ppMP6_0 with nearly zero interval between main injection. The timing of the first photo is set to be the timing when the post injection of ppMP6_0 starts. When the post injection is not introduced, the tail of the main flame can be observed from 7.2 to 7.6°ATDC as illustrated by white circles. When post injection is applied, it could be observed that the tip of the post spray overlapped with the tail of main flame (white dotted circle). When the overlap happens, the ignition timing of the post spray is supposed to be advanced. Consequently, the post spray may not be able to entrain a sufficient amount of air. Even with the additional momentum provided by the post injection, the mixture at the periphery of the combustion chamber will contain more fuel rich region. As a result, the elimination of high temperature gas will be postponed.

The interval between the main spray and post spray could be extended by retarding the post injection timing. In Figure 24, the optical results of ppMP6_0 and ppMP6_1.5 are compared. The starting time was also set to 5.6°ATDC, which is the starting timing of post injection for ppMP6_0. The Figure 24 shows that the post injection started around 7.2°ATDC for ppMP6_1.5. When $\Delta\theta$ was 1.5°CA, the post spray followed the main spray with a certain interval and had contact with the main flame at around 10.4°ATDC at the periphery of the combustion chamber bowl. Allowed with sufficient interval, the air entrainment disruption effect by spray overlapping will be mitigated. As a result, the homogenization of the high temperature gas near chamber edge may be accelerated compared with when $\Delta\theta$ was near zero.

As indicated in the previous section, since the diameter of the combustion was larger for metal engine, the main flame and post spray may have a contact at later timing compared to the timing observed in optical results (Figure 23 and Figure 24). In addition, with near zero interval, the injection mass ratio of main and post injection was smaller for optical engine experiments. Therefore, the combustion phase observed in optical engine experiments may differ from that of metal engine experiments. However, since the injection timing and duration was set to be the same, overall, the following trends are supposed to be the same. First, when the $\Delta\theta$ is small, the air entrainment of the post spray will be disrupted due to the main flame. Second, this phenomenon will be mitigated when $\Delta\theta$ is extended.

At last, the optical results of ppMP6_1.5 were compared with that of ppMP6_4.7 in Figure 25. The starting photo was set at 7.2°ATDC, which is the starting timing of post injection for ppMP6_1.5. When $\Delta\theta$ was extended to 4.7°CA, the start of post injection could be observed at 11.4°ATDC. At this moment, the main flame was concentrate on the periphery of the combustion chamber. The post flame then reached the chamber wall at around 15.2°ATDC. At that time, the main flame could be merely observed. Therefore, the interaction of main flame with post spray was avoided. As a result, longer $\Delta\theta$ lead to an extension of the contact duration of high temperature flame with the chamber wall.

In summary, the optical results showed that when $\Delta\theta$ was increased from 0°CA to 1.5°CA, the post spray may acquire enough interval to entrain more air. When post injection timing is further retarded, the main and post flame interact with the chamber wall and cause heat loss individually. With the same $\Delta\theta$ and spray tip penetration rate for metal and optical experiments, we could expect that the same effect of $\Delta\theta$ could be confirmed for metal engine experiments. For metal engine experiments, the insufficient air entrainment of post spray caused by near zero $\Delta\theta$ could increase the dwell duration of fuel rich high temperature gas near the chamber wall. This could be one reason for the higher cooling loss with $\Delta\theta$ equals to zero shown in Figure 16. In addition, when $\Delta\theta$ is extended, the individual heat loss of main and post flame could also extend the dwell duration of high temperature gas. As a result, the heat loss may increase as shown in Figure 16. As we mentioned previously, in the optical engine experiments, the main injection rate was obviously lower than metal engine experiments (Figure 10). The main flame may remain at the periphery of the combustion chamber for a longer duration. As a result, retarding post injection timing may not that effective on the extension of the contact duration of high temperature gas with the chamber wall. Therefore, as shown in Figure 16, the increase of cooling loss by extending $\Delta\theta$ from 1.5°CA to 4.7°CA may not that obvious for metal engine experiments compared to what was inferred by optical experiments.

As for the experimental results with various intake pressure shown in Figure 20, we can draw the following inferences from the optical experimental results. When the in-cylinder density is high, the main spray entrains sufficient air at the early stage and the high temperature region eliminated early. Therefore, less heat is considered to be transferred from the chamber wall by the main flame. In addition, due to the faster fuel air mixing, the occurrence of fuel rich region due to the overlap of main flame and post spray is reduced. In addition, since the amount of air entrainment by post injection increased regardless of the $\Delta\theta$, the cooling loss amount showed little changes with the different $\Delta\theta$ in Figure 20.

5. Conclusions

In this study, the effects of close post injection strategy on performance, cooling loss, and emissions were investigated using a single-cylinder metal engine. The injection timing of the post injection was modified so that it could range from near zero interval with main injection to a short interval between the main injection. Also, the effects of post injection quantity and intake pressure were investigated. Then, an optical engine was used to investigate the combustion characteristics of post injection. The conclusions are summarized below.

1. The results of metal engine experiments showed that the cooling loss could be reduced by applying close post injection. The reduction of main spray impingement on the chamber wall is considered as one reason for this reduction.

2. With close post injection, the cooling loss is reduced and the change of DCV was small, therefore, the thermal efficiency was improved.

3. By retarding post injection timing slightly from near zero interval between the

main injection, the cooling loss showed a decrease. Further retarding post injection could not decrease the cooling loss constantly.

4. The optical experiments showed the air entrainment of the post spray is suppressed by the existence of the tail of the main spray when the injection interval is too short. Due to this disruption, a fuel rich region will be formed near the chamber wall. As a result, the high temperature gas will remain near the wall for longer duration and cause higher cooling loss. The slightly later post injection timing mitigates the interaction, which would lead to reduced cooling loss.

5. A similar tendency of cooling loss against the injection interval was observed when the post-injection quantity was varied from 3 mm^3/cycle to 15 mm^3/cycle.

6. When the intake pressure was high, the reduction of cooling loss due to post injection was small. Therefore, the effect of thermal efficiency improvement was small.

Acknowledgements

The authors would like to thank Masayoshi Furukawa and Tomoki Taguchi for their valuable assistance during the experiments. In addition, a part of work was supported by Sasahara Foundation for the Promotion of Engineering.

References

1. Walker, Andy. Future challenges and incoming solutions in emission control for heavy duty diesel vehicles. Topics in Catalysis 59.8-9 (2016): 695-707.
2. Zamboni, Giorgio, Simone Moggia, and Massimo Capobianco. Hybrid EGR and turbocharging systems control for low NOX and fuel consumption in an automotive diesel engine. Applied energy 165 (2016): 839-848.
3. Guerrassi, N., and P. Dupraz. A common rail injection system for high speed direct

injection diesel engines. SAE Technical Paper, 980803, 1998.

4. Ueda, Daiji, et al. 4th Generation Diesel Piezo Injector (Realizing Enhanced High Response Injector). SAE Technical Paper, 2016-01-0846, 2016.
5. Badami, Marco, et al. Influence of multiple injection strategies on emissions, combustion noise and BSFC of a DI common rail diesel engine. SAE Transactions (2002): 1118-1129.
6. Okude, Keiichi, et al. Effects of multiple injections on diesel emission and combustion characteristics. SAE Technical Paper, 2007-01-4178, 2007.
7. Arrègle, Jean, et al. Insights on postinjection-associated soot emissions in direct injection diesel engines. Combustion and flame 154.3 (2008): 448-461.
8. Horibe, Naoto, et al. Smoke- Reduction Effect of After Injection in Combination with Pilot Injection. Transactions of Society of Automotive Engineers of Japan. 2012, Vol.43, No.5, p.1039-1044.
9. Benajes, Jesus, Santiago Molina, and José M. García. Influence of pre-and post-injection on the performance and pollutant emissions in a HD diesel engine. SAE Transactions (2001): 361-371.
10. Payri, F., Benajes, J., Pastor, J., and Molina, S., “Influence of the Post Injection Pattern on Performance, Soot and NOx Emissions in a HD Diesel Engine,” SAE Technical Paper 2002-01-0502, 2002.
11. Hotta, Y., Inayoshi, M., Nakakita, K., Fujiwara, K. et al., “Achieving Lower Exhaust Emissions and Better Performance in an HSDI Diesel Engine with Multiple Injection,” SAE Technical Paper 2005-01-0928, 2005.
12. Desantes, José M., et al. A comprehensive study of diesel combustion and emissions with post-injection. SAE Technical Paper, 2007-01-0915, 2007.

13. Horibe, N., Bao, Z., Taguchi, T., Egoshi, K. et al., Improvement of Thermal Efficiency in a Diesel Engine with High-Pressure Split Main Injection. SAE Technical Paper, 2018-01-1791, 2018.

14. Osada, Hideaki, Yuzo Aoyagi, and Kazuaki Shimada. Diesel Combustion Improvement Using High Boost, Wide Range and High Rate EGR in a Single Cylinder Engine (Third Report). Transactions of Society of Automotive Engineers of Japan 43.4 (2012).

15. Kazuki, I., Yosuke, M., Yanhe, Z., et al., Thermal Efficiency Improvements with Split Primary Fuel Injections in Semi-Premixed Diesel Combustion with Multi-Peak Shaped Heat Releas. SAE Technical Paper 2019-01-2170, 2019.

16. O'Connor, Jacqueline, and Mark Musculus. Optical investigation of the reduction of unburned hydrocarbons using close-coupled post injections at LTC conditions in a heavy-duty diesel engine. SAE International Journal of Engines 6.1 (2013): 379-399.

17. O'Connor, Jacqueline, Mark PB Musculus, and Lyle M. Pickett. Effect of post injections on mixture preparation and unburned hydrocarbon emissions in a heavy-duty diesel engine. Combustion and Flame 170 (2016): 111-123.

18. Bowditch, Fred W. A new tool for combustion research a quartz piston engine. SAE Technical Paper, 610002, 1961.

19. Wakuri, Yutaro, et al. Studies on the penetration of fuel spray in a diesel engine. Bulletin of JSME 3.9 (1960): 123-130.

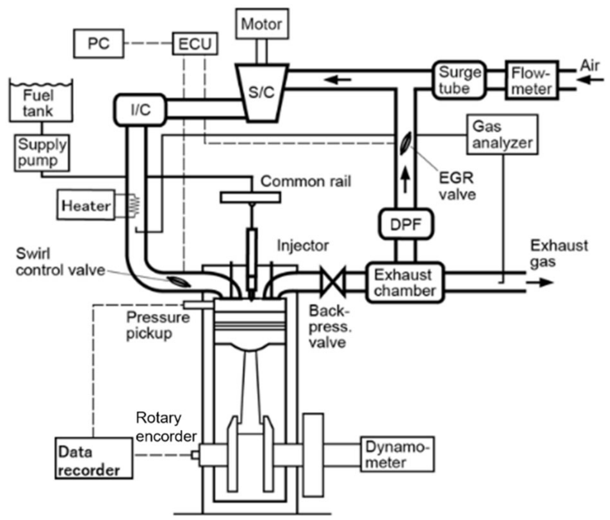

Fig 1. The schematic of experimental setup for the experiments of metal engine.

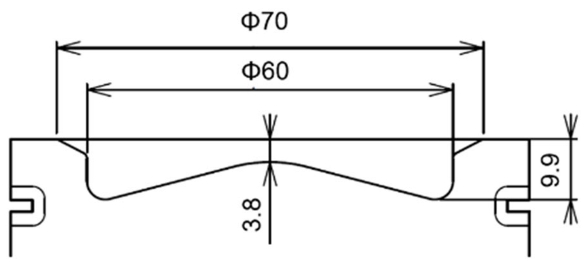

Fig 2. The shape of piston bowl used for metal engine experiments.

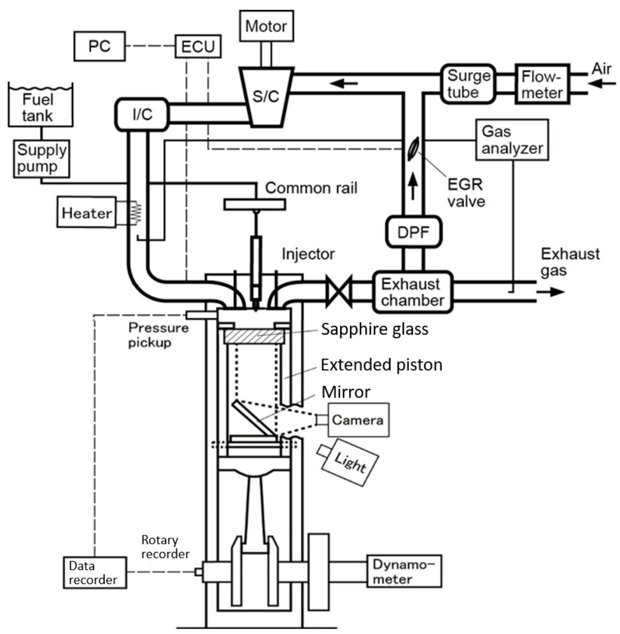

Fig 3. The schematic of experimental setup for the experiments of optical engine.

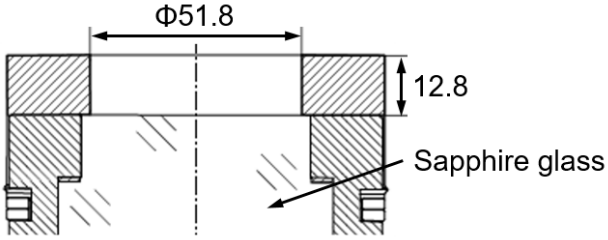

Fig 4. The cross section view of bottom view piston.

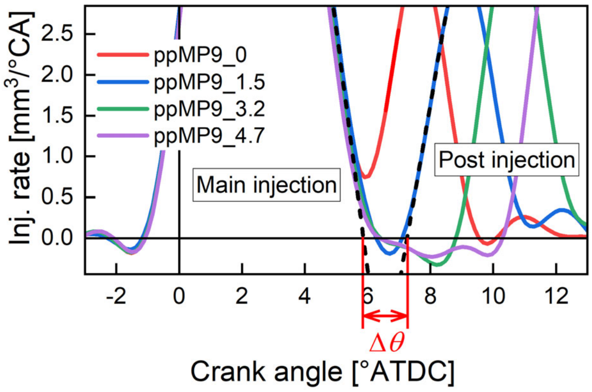

Fig 5. An example of injection rate shape with close post injection and its interval between the main injection.

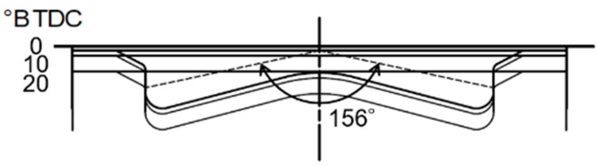

Fig 6. The location of injection axis relative to the piston.

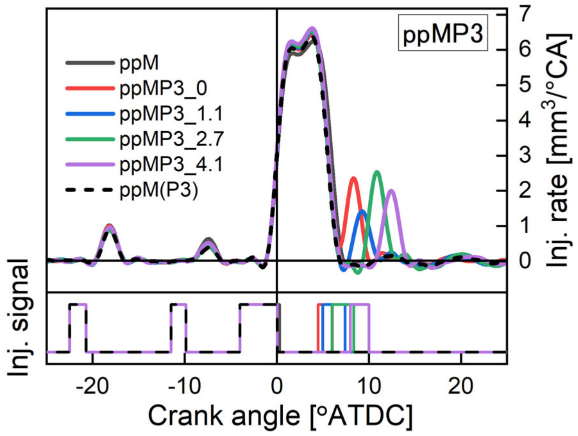

Fig 7. The injection rate with post injection quantity of 3 mm^3/cycle.

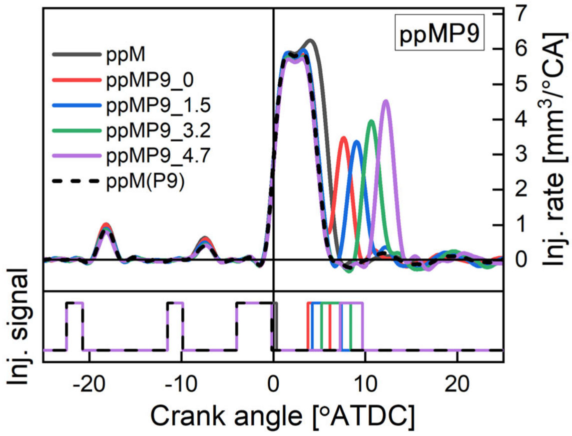

Fig 8. The injection rate with post injection quantity of 9 mm^3/cycle.

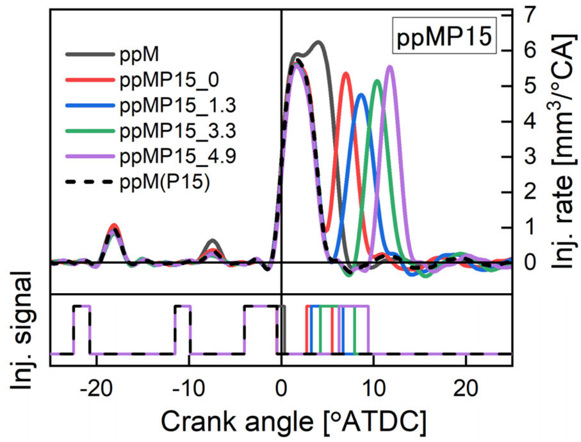

Fig 9. The injection rate with post injection quantity of 15 mm^3/cycle.

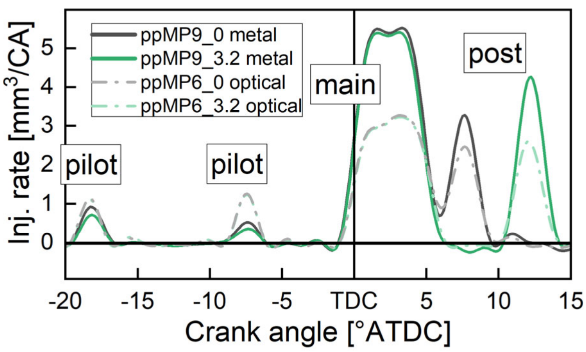

Fig 10. An example of injection rate of metal engine operating condition (solid line) and optical engine operating condition (dashed line).

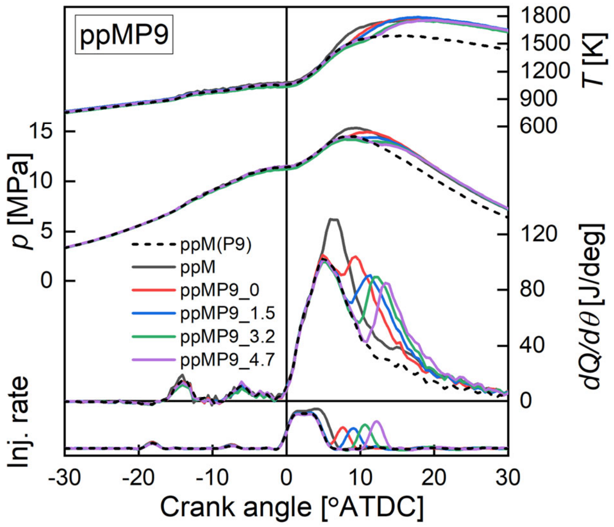

Fig 11. The heat release rate, in-cylinder pressure, and average in-cylinder temperature as function of crank angle when close post injection with quantity of 9 mm^3/cycle was applied.

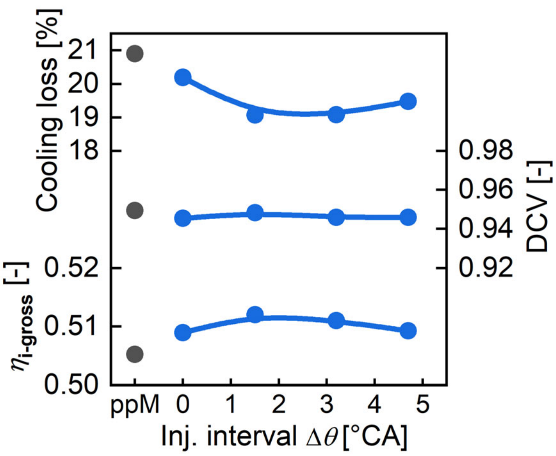

Fig 12. The engine performance against injection interval with post injection 9 mm^3/cycle.

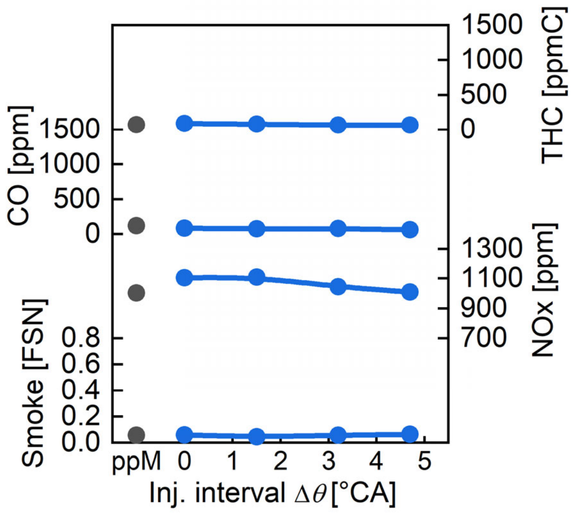

Fig 13. The exhaust emissions against injection interval with post injection 9 mm³/cycle compared.

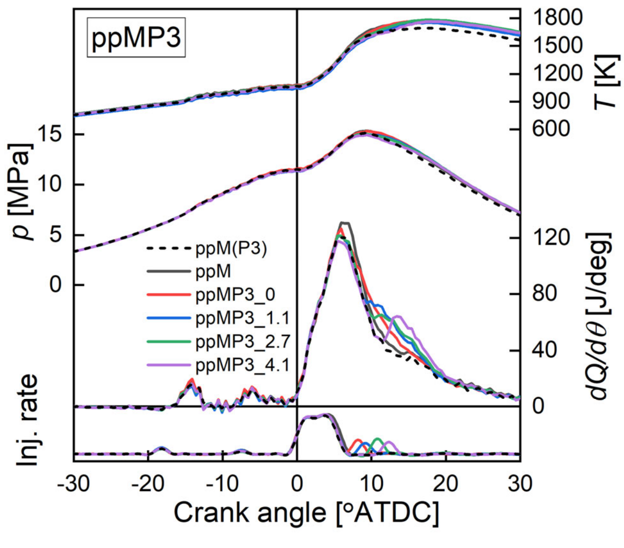

Fig 14. The heat release rate, in-cylinder pressure, and average in-cylinder temperature as function of crank angle when close post injection with quantity of 3 mm³/cycle was applied.

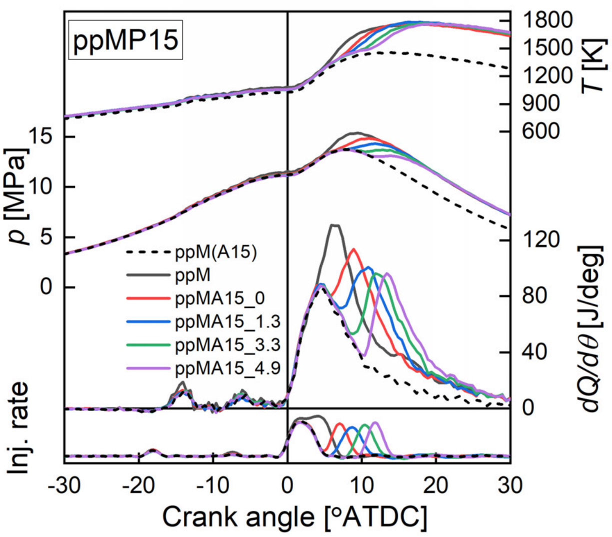

Fig 15. The heat release rate, in-cylinder pressure, and average in-cylinder temperature as function of crank angle when close post injection with quantity of 15 mm³/cycle was applied.

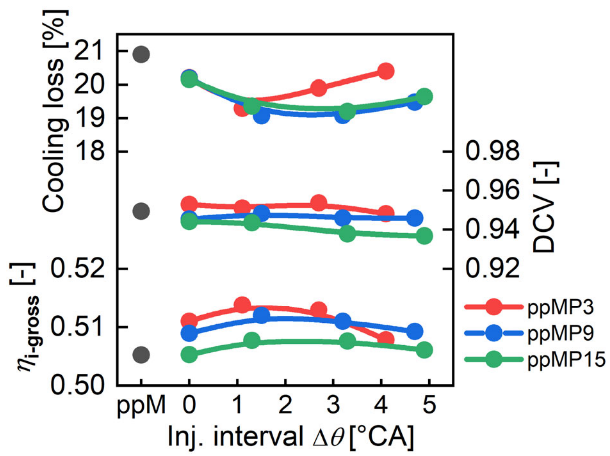

Fig 16. The engine performance against injection interval for different post-injection quantities.

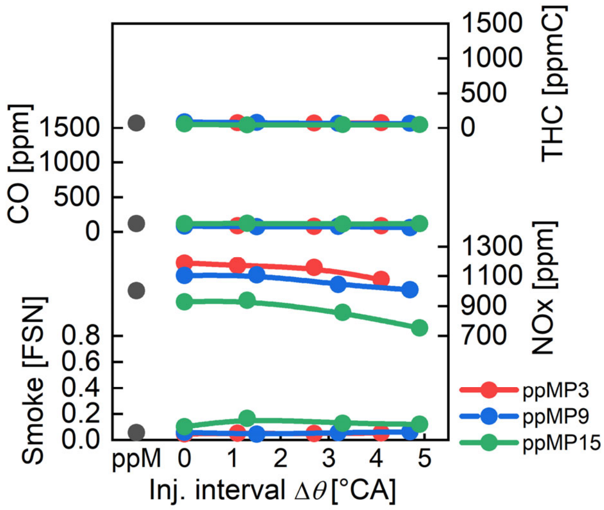

Fig 17. The exhaust emissions against injection interval for different post-injection quantities.

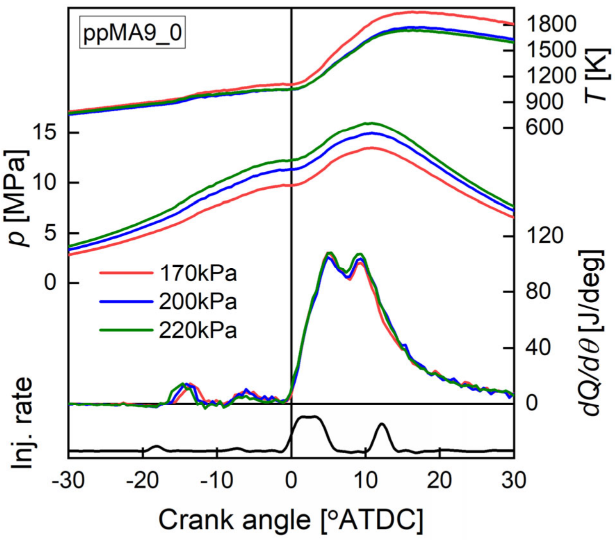

Fig 18. The heat release rate, in-cylinder pressure, and average in-cylinder temperature as function of crank angle when close post injection with various intake pressure was applied (ppMP9_0).

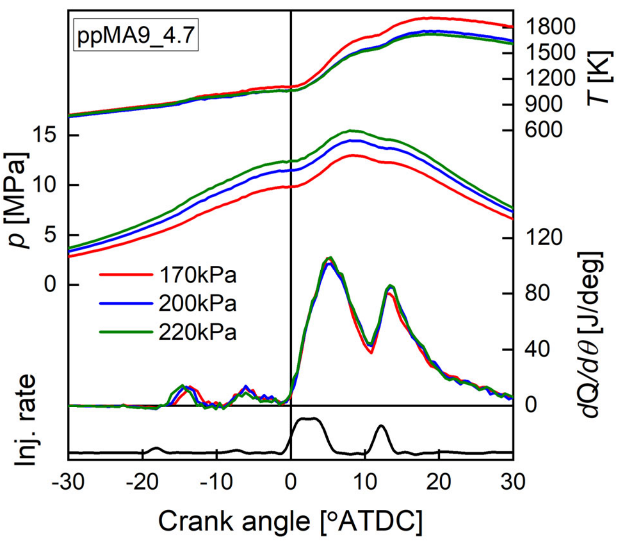

Fig 19. The heat release rate, in-cylinder pressure, and average in-cylinder temperature as function of crank angle when close post injection with various intake pressure was applied (ppMP9_4.7)

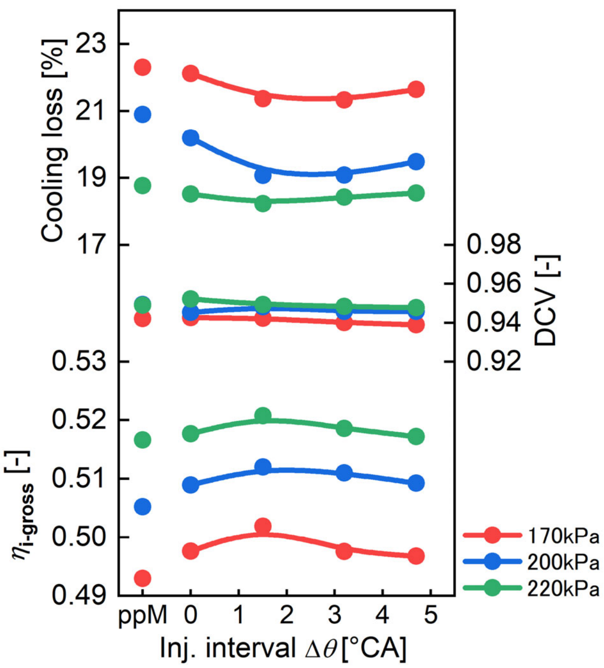

Fig 20. The engine performance against injection interval with various intake pressures.

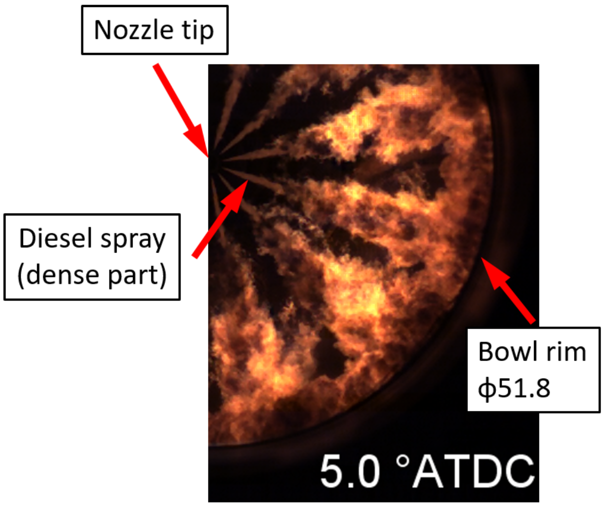

Fig 21. An example of high-speed photograph of spray and flame.

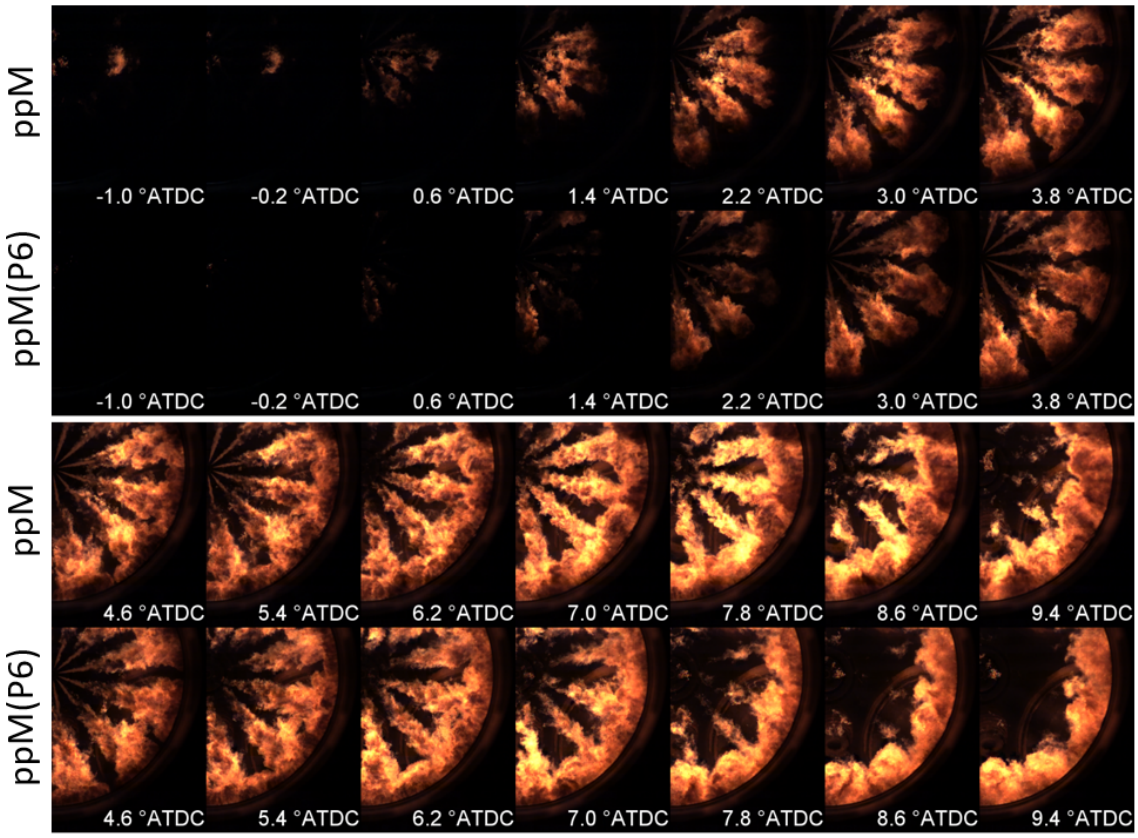

Fig.22 The comparison of spray and flame images between ppM and ppM(P6).

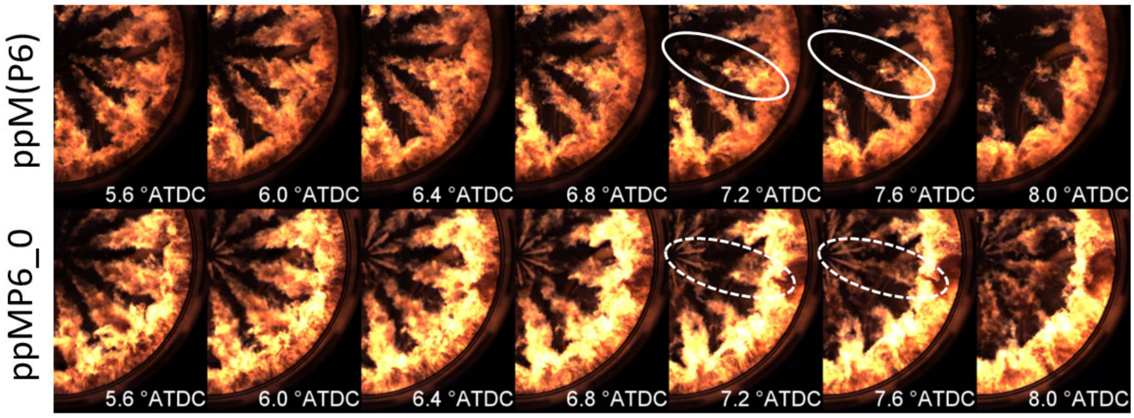

Fig. 23 The comparison of spray and flame images between ppM(P6) and ppMP6_0.

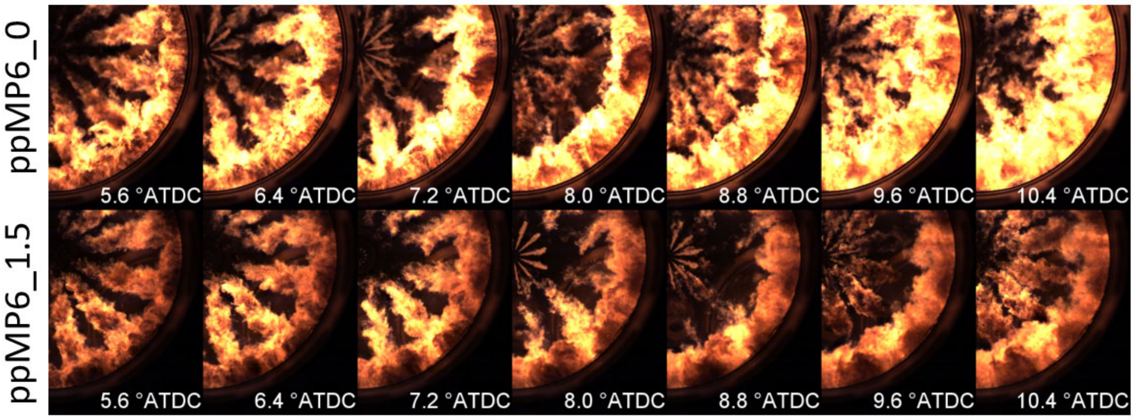

Fig. 24 The comparison of spray and flame images between ppMP6_0 and ppMP6_1.5.

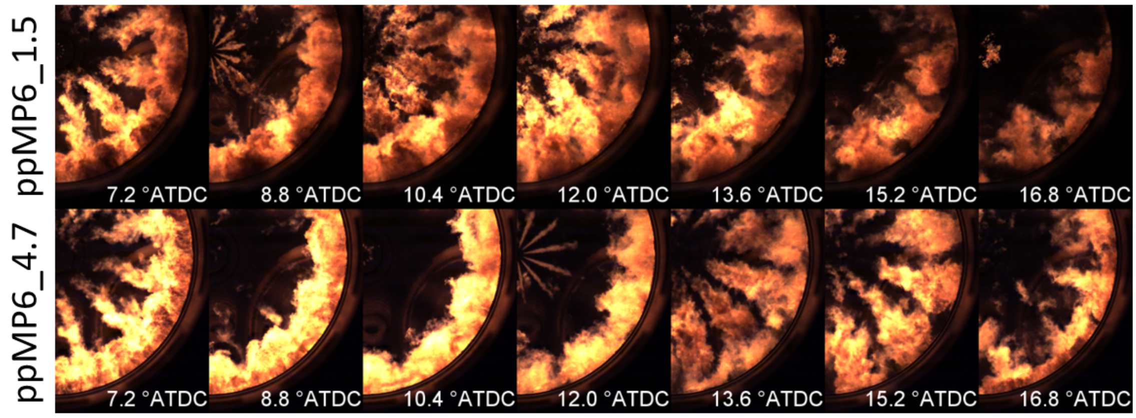

Fig. 25 The comparison of spray and flame images between ppMP6_1.5 and ppMP6_4.7.

Table 1. The major specifications of the engine

Engine type	Direct-injection diesel engine, Single-cylinder, Water-cooled
Bore × Stroke [mm]	85.0 × 96.9
Displacement [cm^3]	550
Injection system	Common-rail system ϕ0.114 mm × 12 holes nozzle 156° included angle
Charging	External supercharging
EGR system	Low-pressure loop EGR

Table 2. The comparison of the operation condition of metal engine and optical engine

	Metal Engine	Optical Engine
Rotational speed [rpm]	2250	2000
Intake pressure [kPa]	200	200
Exhaust pressure [kPa]	200	200
Intake temperature [degC]	50	50
Injector nozzle diameter [mm]	0.114	0.104
Injector nozzle hole number	12	12
Injection pressure [MPa]	270	160
Compression ratio	18.3	15.4
Fuel rate [mm^3/cycle]	39.0	30.0

Table 3. The injection timing and quantity for metal engine operation.

	Injection timing [°ATDC]	Injection quantity [mm^3/cycle]
1st injection	-20.2	1.7
2nd injection	-9.2	1.8
3rd injection	-1.7	35.5, 32.5, 26.5, 20.5
4th injection	Varied	0, 3, 9, 15

Table 4. The intervals between main injection and post injection.

	ppMP3	ppMP9	ppMP15
Intervals between main injection and post injection $\Delta\theta$ [°CA]	0	0	0
	1.1	1.5	1.3
	2.7	3.2	3.3
	4.1	4.7	4.9